J. Fluid Mech. (1969), vol. 35, part 3, pp. 599–608
Printed in Great Britain

Mass flow rate for nearly-free molecular slit flow

By J. DANIEL STEWART
Aerospace Corporation El Segundo, California

(Received 18 April 1968)

The local and average mass flow rates for nearly free molecular flow through a two-dimensional slit are determined for several tank pressure ratios. The equilibrium gas in the two tanks and the container walls are assumed to be at the same temperature and the Willis iterative method with the Bhatnager–Gross–Krook model is used for the analysis. The results for an infinite pressure ratio are also presented in order to illustrate the effects of a finite pressure ratio.

1. Introduction

Liepmann (1960) has pointed out that orifice or slit flow offers the possibility of comparing theory and experiment without having to assume a particular gas-wall interaction model. The local and average mass flow rates for these two flow problems have been determined theoretically by Willis (1965) for the case of an infinite pressure ratio. Previously, Narasimha (1961) had obtained an expression for the average mass flow rate based on the centreline value for a circular orifice. Both authors used the Willis (1958) iterative method. The purpose of the present work is to determine the effects of a finite pressure ratio on the local and average mass flow rates for nearly free molecular flow through a two-dimensional slit for an isothermal system , i.e. the equilibrium gas temperatures in the two tanks and the container wall temperature are assumed to be equal. The Willis iterative method is also used here.

The physical problem considered in this paper consists of the flow of gas between two reservoirs which, respectively, contain gas in equilibrium with temperature T and pressures p_1 and p_2, as shown in figure 1. The opening between the two reservoirs is in the form of a two-dimensional slit and the walls separating the two reservoirs are of infinitesimal thickness. The velocity distribution function in each reservoir is assumed to be the Maxwellian distribution function corresponding to the appropriate reservoir densities and temperature.

2. Analysis

Iterative form of the Boltzmann equation

Willis's iterative form for the Boltzmann equation for a finite total collision cross-section can be expressed as follows:

$$f^{(1)}(\mathbf{s},\xi_r) = f(\mathbf{s}_0,\xi_r) + \int_{\mathbf{s}_0}^{\mathbf{s}} \frac{ds'}{\xi_r}[P^{(0)}(\mathbf{s}') - f(\mathbf{s}_0,\xi_r)D^{(0)}(\mathbf{s}')]\exp\left(-\int_{\mathbf{s}'}^{\mathbf{s}} \frac{D^{(0)}(\mathbf{s}'')}{\xi_r}ds''\right), \quad (1)$$

where $f(\mathbf{s}, \boldsymbol{\xi}_r)$ is the local velocity distribution function, $\mathbf{s}$ is the spatial vector, $\boldsymbol{\xi}_r$ is the molecular velocity in the (x, y)-plane, and ds' and ds'' are differential quantities measured along the line specified by the angle α, as illustrated in figure 1. The superscripts (1) and (0) denote the first and zeroth iterations, respectively;

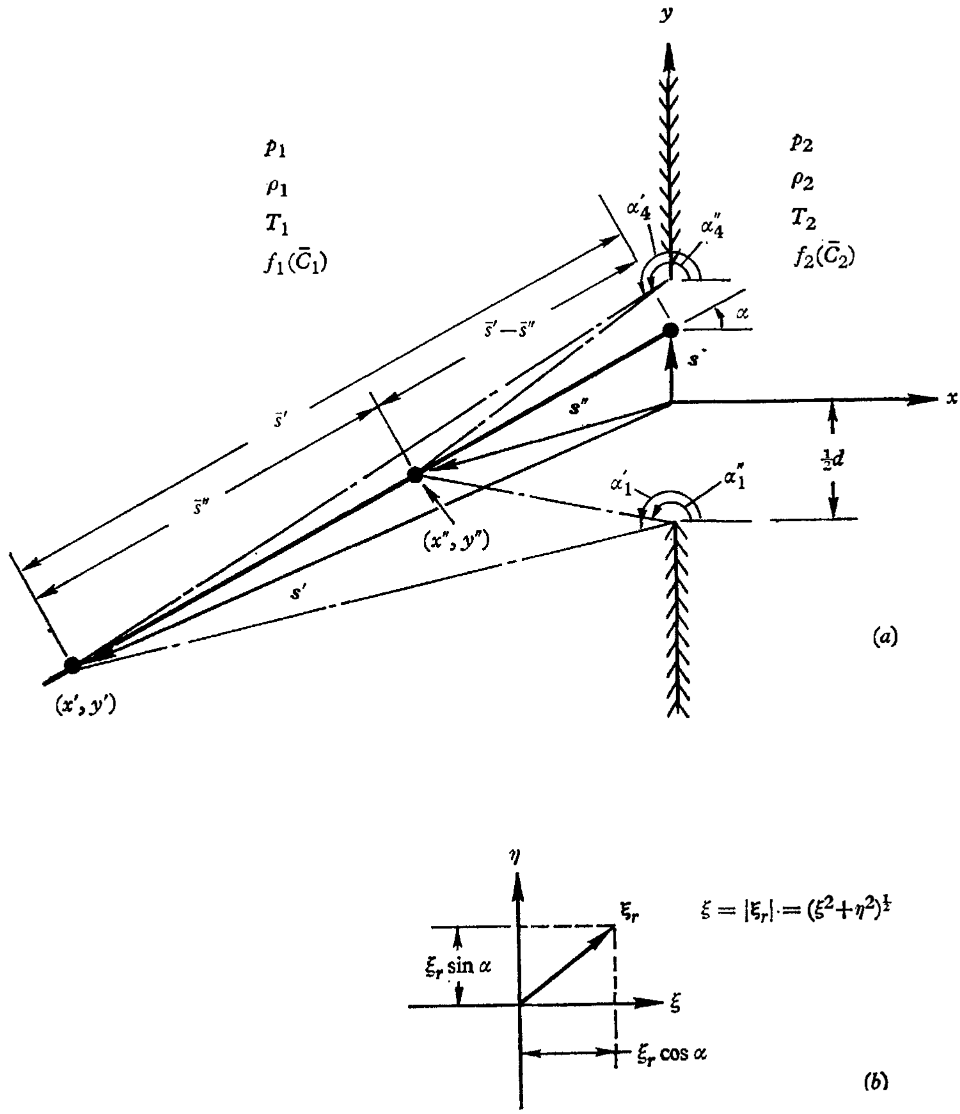

FIGURE 1. (a) Schematic diagram of the two-dimensional slit. (b) Illustration of velocity co-ordinate system.

the zeroth iteration is the free-molecular solution. The functions $P^{(0)}(\mathbf{s}')$ and $f(\mathbf{s}_0, \boldsymbol{\xi}_r) D^{(0)}(\mathbf{s}')$ represent the production and loss, respectively, of molecules with velocity $\boldsymbol{\xi}_r$ due to collisions, and the molecular speed is denoted by ξ_r. The vector $\mathbf{s}_0$ represents a point on the boundary and $f(\mathbf{s}_0, \boldsymbol{\xi}_r)$ is the corresponding distribution function. The boundary distribution functions are taken as the

Maxwellian equilibrium distribution functions for the tanks. These are given by

$$f(s_0 = \infty, \alpha, \xi_r, \zeta) = n_i(2\pi RT_i)^{-\frac{3}{2}} \exp\left[-(\xi^2+\eta^2+\zeta^2)/2RT_i\right], \tag{2}$$

where n_i and T_i are the number density and temperature, respectively, and are equal to n_1 and T_1 for $-\frac{1}{2}\pi \leqslant \alpha \leqslant \frac{1}{2}\pi$ and n_2 and T_2 for $\frac{1}{2}\pi \leqslant \alpha \leqslant \frac{3}{2}\pi$, R is the gas constant, and ξ, η, and ζ are the molecular velocity components in the x-, y- and z-directions, respectively. The assumption of an isothermal system (i.e. $T_1 = T_2$) will be delayed until later. Polar co-ordinates s' and α with origin at $x = 0$ and y, as illustrated in figure 1, have been introduced and the boundary condition is satisfied at infinity for simplicity. It should be noted that for rays specified by α such that the container walls which lie in the plane of the slit are approached, the boundary condition given by (2) is still applied. It can be shown that the limiting case in which the rays coincide with the container walls is not important since there is no contribution to the mass flow for the first iteration.

The evaluation of $P^{(0)}(\mathbf{s}')$ and $D^{(0)}(\mathbf{s}')$ can be greatly simplified by replacing the Maxwell–Boltzmann collisional operator with the simple statistical operator suggested by Bhatnager, Gross & Krook (1954):

$$D^{(0)}(\mathbf{s}') = \nu n^0 \tag{3}$$

and

$$P^{(0)}(\mathbf{s}') = \nu n^{0^2}(h^0/\pi)^{\frac{3}{2}} \exp\left[-h^0(\boldsymbol{\xi}_r - \mathbf{w}^0)^2\right], \tag{4}$$

where $h^0 = (2RT^0)^{-1}$, ν is a constant, and n^0, $\mathbf{w}^0$ and T^0 are the free-molecular values for the local number density, macroscopic velocity, and temperature, respectively.

It is convenient to introduce the following definitions:

$$N_i^0 \equiv n^0/n_i, \qquad B_i^0 \equiv h^0/h_i, \qquad \mathbf{C}_i \equiv h_i^{\frac{1}{2}}\boldsymbol{\xi}_r, \tag{5a}$$

$$\mathbf{W}_i^0 \equiv h_i^{\frac{1}{2}}\mathbf{w}^0, \qquad C_i^2 \equiv h_i\xi_r^2, \qquad \bar{C}_i^2 \equiv h_i(\xi_r^2+\zeta^2), \tag{5b}$$

$$\delta_i \equiv \nu n_i h_i^{\frac{1}{2}}\tfrac{1}{2}d, \quad h_i^{-\frac{1}{2}} \equiv (2RT_i)^{\frac{1}{2}}, \quad \bar{s}' \equiv \frac{|\mathbf{s}-\mathbf{s}'|}{d}, \tag{5c}$$

where the subscript is either 1 or 2 denoting the upstream and downstream tanks, respectively. The parameter δ_i is the inverse Knudson number based on one-half the slit width, $\frac{1}{2}d$. Narasimha (1961) has determined the constant ν by requiring the collision frequency per unit volume in the undisturbed gas to be consistent with the B-G-K model. Willis (1965) introduced the Chapman–Enskog viscosity to show that this leads to

$$\delta_i = Re_i/2\sqrt{2}. \tag{6}$$

Since moments of equation (1) are of interest, simplification can be made by integrating the molecular velocity component in the z-direction over the full range (i.e. $-\infty$ to $+\infty$). Thus, define

$$F_i^{(1)}(\bar{y}, \alpha, C_i) \equiv \frac{1}{\sqrt{\pi}}\int_{-\infty}^{\infty} f_i^{(1)}(\bar{y}, \alpha, \bar{C}_i)\, h_i^{\frac{1}{2}}\, d\zeta \tag{7}$$

and

$$F_i(C_i) \equiv n_i(2\pi RT_i)^{-1}\exp(-C_i^2), \tag{8}$$

where $i = 1$ for $-\frac{1}{2}\pi \leqslant \alpha \leqslant \frac{1}{2}\pi$ and $i = 2$ for $\frac{1}{2}\pi \leqslant \alpha \leqslant \frac{3}{2}\pi$. Combining equations (1) to (6) and letting $s_0 \to \infty$, the first iteration for the reduced distribution function can be expressed as

$$F_i^{(1)}(\bar{y},\alpha,C_i) = F_i(C_i)\left\{1+\frac{Re_i}{\sqrt{2}}\int_0^\infty \frac{d\bar{s}'}{C_i} N_i^0(\bar{s}',\alpha)\,[N_i^0(\bar{s}',\alpha)\,B_i^0(\bar{s}',\alpha)\right.$$

$$\times \exp\left(-B_i^0(\bar{s}',\alpha)\,[C_i^2-2\mathbf{C}_i\,.\,\mathbf{W}_i^0(\bar{s}',\alpha)+W_i^0(\bar{s}',\alpha)^2]+C_i^2\right)-1]$$

$$\left.\times \exp\left(-\frac{Re_i}{\sqrt{2}}\int_0^{\bar{s}'}\frac{N_i^0(\bar{s}'',\alpha)}{C_i}\,d\bar{s}''\right)\right\}. \quad (9)$$

It should be noted that $N_i^0(\bar{s}',\alpha)$, $B_i^0(\bar{s}',\alpha)$, etc., are also functions of $\bar{y}$, the non-dimensional spatial co-ordinate, which is given by y/d. Equation (9) can be applied directly to determine the local mass flow rate from the appropriate velocity moment.

Local and average mass flow rates

The local flow rate is defined as follows:

$$\dot{m}^{(1)}(\bar{y}) \equiv n^{(1)}(x=0,\bar{y})\,u^{(1)}(x=0,\bar{y}) = \tfrac{1}{2}\pi\int_0^\infty\int_0^{2\pi} \xi F^{(1)}(\bar{y},\alpha,C_i)\,\xi_r\,d\alpha\,d\xi_r. \quad (10)$$

Introducing (9) with $i=1$ for $-\frac{1}{2}\pi \leqslant \alpha \leqslant \frac{1}{2}\pi$ and $i=2$ for $\frac{1}{2}\pi \leqslant \alpha \leqslant \frac{3}{2}\pi$, the local flow rate can be expressed as the sum of the upstream and downstream flows; that is

$$\dot{m}^{(1)}(\bar{y}) = \dot{m}_1^{(1)}(\bar{y})+\dot{m}_2^{(1)}(\bar{y}), \quad (11)$$

where $\dot{m}_1^{(1)}(\bar{y})$ and $\dot{m}_2^{(1)}(\bar{y})$ are defined as follows:

$$\dot{m}_1^{(1)}(\bar{y}) \equiv \pi^{\frac{1}{2}}h_1^{-2}\int_0^\infty\int_{-\frac{1}{2}\pi}^{\frac{1}{2}\pi} F_1^{(1)}(\bar{y},\alpha,C_1)\,C_1^2\cos\alpha\,d\alpha\,dC_1, \quad (12)$$

$$\dot{m}_2^{(1)}(\bar{y}) \equiv \pi^{\frac{1}{2}}h_2^{-2}\int_0^\infty\int_{\frac{1}{2}\pi}^{\frac{3}{2}\pi} F_2^{(1)}(\bar{y},\alpha,C_2)\,C_2^2\cos\alpha\,d\alpha\,dC_2. \quad (13)$$

The average mass flow rate through the slit can then be obtained by averaging the local values across the slit. Making the assumption of an isothermal system the Reynolds number based on the downstream flow properties, Re_2, can be related to the upstream Reynolds number, Re_1, by the product of the pressure ratio.

Free-molecular solution

The free-molecular solution for a two-dimensional slit can be obtained as a limiting case from the solution given by Stewart (1967) for two-dimensional channels of arbitrary length. The results are as follows:

$$N_1^0(\bar{s}',\alpha)\,U_1^0(\bar{s}',\alpha) = (1-p_2/p_1)\,(\sin\alpha_1'-\sin\alpha_4')/4\pi^{\frac{1}{2}}, \quad (14)$$

$$N_1^0(\bar{s}',\alpha)\,V_1^0(\bar{s}',\alpha) = (1-p_2/p_1)\,(\cos\alpha_4'-\cos\alpha_1')/4\pi^{\frac{1}{2}}, \quad (15)$$

$$B_1^0(\bar{s}',\alpha) = \{1-\tfrac{2}{3}[U_1^0(\bar{s}',\alpha)^2+V_1^0(\bar{s}',\alpha)^2]\}^{-1}, \quad (16)$$

$$N_1^0(\bar{s}',\alpha) = (1-p_2/p_1)\,[j-(\alpha_4'-\alpha_1')/2\pi]+p_2/p_1, \quad (17)$$

where $j=0$ for $0 \leqslant \alpha_4 \leqslant \frac{1}{2}\pi$ and $j=1$ for $\frac{1}{2}\pi \leqslant \alpha_4 \leqslant 2\pi$. The angles α_4' and α_1' are illustrated in figure 1 and are given by the following expressions:

$$\tan\alpha_1' = [\bar{s}'\sin\alpha - (\bar{y}+\tfrac{1}{2})]/\bar{s}'\cos\alpha, \tag{18}$$

$$\tan\alpha_4' = [\bar{s}'\sin\alpha - (\bar{y}-\tfrac{1}{2})]/\bar{s}'\cos\alpha. \tag{19}$$

The expressions for α_1'' and α_4'', as shown in figure 1, can be obtained from (18) and (19) by replacing $\bar{s}'$ with $(\bar{s}'-\bar{s}'')$.

Evaluation of the integrating factor

Introducing (17) into the integral of the integrating factor, as given in (9), and performing the integrations yield

$$\int_0^{\bar{s}'} N_1^0(\bar{s}'',\alpha)\,d\bar{s}'' = (1-p_2/p_1)\{j\bar{s}' - [E(\bar{s}',\alpha)-D(\bar{s}',\alpha)]/2\pi\} + \bar{s}'p_2/p_1, \tag{20}$$

where $j = 1$ for $-\frac{1}{2}\pi \leqslant \alpha \leqslant \frac{1}{2}\pi$ and $j = 0$ for $\frac{1}{2}\pi \leqslant \alpha \leqslant \frac{3}{2}\pi$, and

$$\begin{aligned} E(\bar{s}',\alpha) = {} & \tfrac{1}{2}(\bar{y}-\tfrac{1}{2})\{\cos\alpha\,[2\ln|\bar{y}-\tfrac{1}{2}| - \ln|[\bar{s}'\sin\alpha-(\bar{y}-\tfrac{1}{2})]^2 \\ & + \bar{s}'^2\cos^2\alpha|] - 2\sin\alpha[\tan^{-1}(\tan\alpha) + \tan^{-1}([\bar{s}'-(\bar{y}-\tfrac{1}{2})\sin\alpha]/(\bar{y}-\tfrac{1}{2})\cos\alpha)]\} \\ & + \bar{s}'\tan^{-1}([\bar{s}'\sin\alpha-(\bar{y}-\tfrac{1}{2})]/\bar{s}'\cos\alpha). \end{aligned} \tag{21}$$

The expression for $D(\bar{s}',\alpha)$ can be obtained from (21) by replacing $(\bar{y}-\frac{1}{2})$ with $(\bar{y}+\frac{1}{2})$.

Evaluation of the remaining integrals

The only integrals encountered in evaluating $\dot{m}_1^{(1)}(\bar{y})$ and $\dot{m}_2^{(1)}(\bar{y})$ which offered more than routine difficulties were of the form

$$I_n(a,b) \equiv \int_0^\infty x^n \exp(+bx - ax - x^2)\,dx. \tag{22}$$

By comparing (9), (12) and (13), it can be seen that this type of integral occurs when the integrations with respect to molecular speed are performed.

For the case where $b = 0$ and $a \geqslant 0$, the integral given by (22) can be evaluated with an error of less than $\pm 2\times 10^{-6}$ by using the expressions given by Willis (1960). For the case when $b \neq 0$ and $a \geqslant 0$, the integral can be evaluated by a method given also by Willis (1964). The results obtained by this method for $0 \leqslant a \leqslant 20$ and $-2 \leqslant b \leqslant 2$ were compared with the numerical results of Chahine & Narasimha (1963) for $n = 0$, 1 and 2, and found to be in good agreement. The latter results are reported to be accurate to better than eight places. For the problem considered here, the range of b was $-2{\cdot}0 < b < 1{\cdot}2$. Thus, based on the results of the comparison discussed above for this range, the method of Willis provided accurate results. This comparison is discussed in greater length by Stewart (1967) and numerical values for the results of the comparison are presented.

The remaining integrals were evaluated by numerical quadrature. The Gauss–Laguerre quadrature was used for part of the $\bar{s}'$ integration, and the regular Gauss quadrature was used for the remainder of the $\bar{s}'$ integration and the

α integration. Since the integrand has a sharp peak for small $\bar{s}'$ and asymptotically approaches zero for larger $\bar{s}'$, it was found that very accurate results could be obtained by dividing the $\bar{s}'$ integration into two parts. Finally, the average flow rate was determined by applying a Simpson integration for the local values at five points across half of the slit.

3. Results

The results for the local mass flow rate are presented in figure 2 for pressure ratios of 2, 100 and infinity, and Reynolds numbers ranging from zero to 6·4. The local flow rate is non-dimensionalized with the constant free-molecular flow rate $(\dot{m}_1^{\text{f.m.}} - \dot{m}_2^{\text{f.m.}})$, and is presented for only one-half of the slit. For very small Reynolds numbers the local flow rate is almost constant across the entire slit. For larger Reynolds numbers the local flow rate is still essentially constant near the centre of the slit, but near the edge of the slit it drops off rapidly due to the shielding effect of the slit walls. The results for the infinite pressure ratio, as shown in figure 2 (*c*), were compared with the graphical results of Willis (1965). The agreement was good everywhere except at the edge of the slit, where the results differed by as much as approximately 15 % for a Reynolds number of 6·4. For the smaller Reynolds numbers of 3·2, 1·6, 0·64 and 0·32, the results differed by 4·3, 4·0, 2·0 and 2·2 %, respectively. It should be noted, however, that the

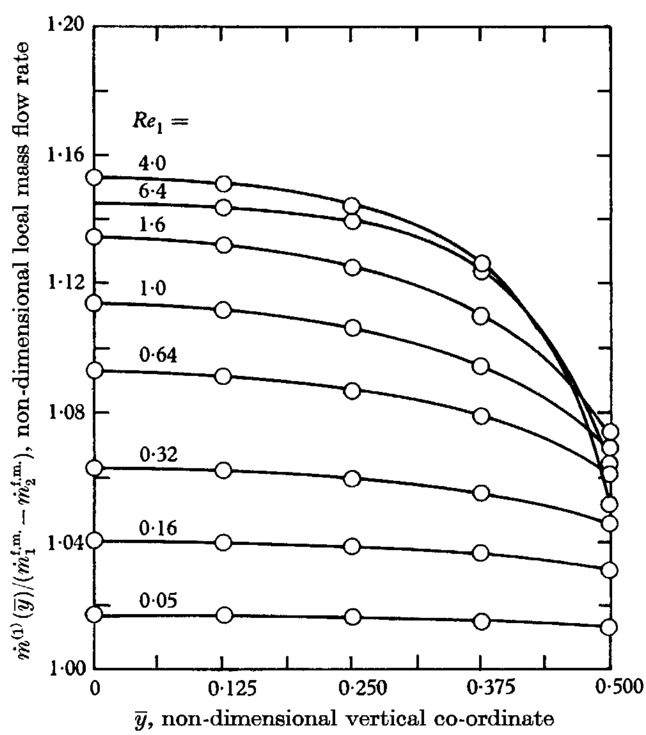

FIGURE 2(*a*). Non-dimensional local mass flow rate for various Reynolds numbers and a pressure ratio, $p_1/p_2 = 2 \cdot 0$. ○, calculated points.

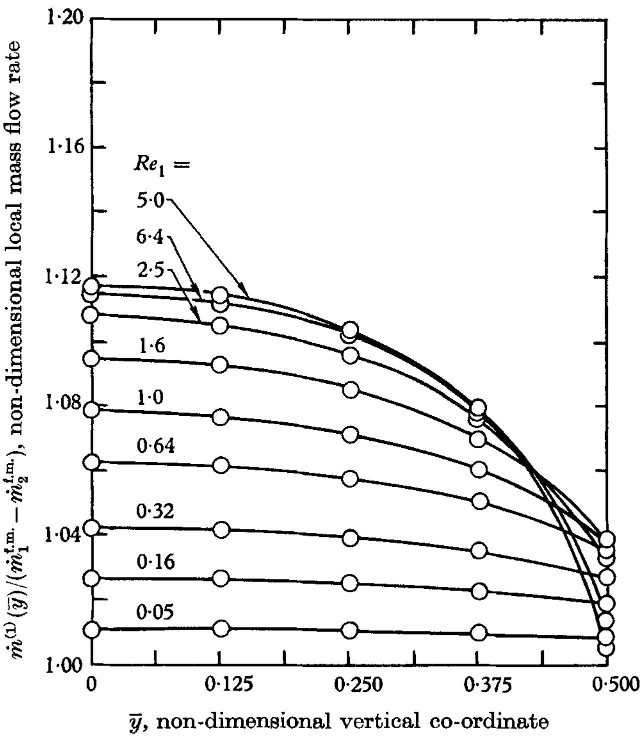

FIGURE 2(*b*). Non-dimensional local mass flow rate for various Reynolds numbers and a pressure ratio, $p_1/p_2 = 100$. ○, calculated points.

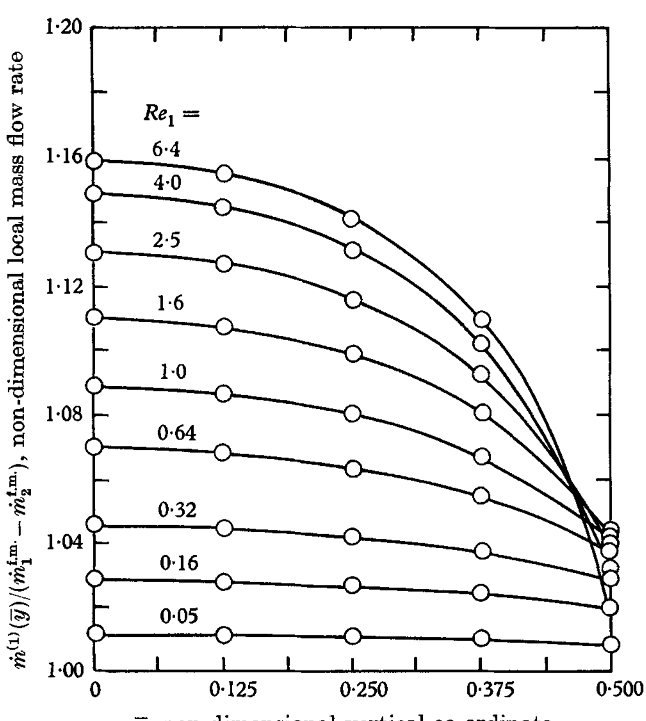

FIGURE 2(*c*). Non-dimensional local mass flow rate for various Reynolds numbers and a pressure ratio, $p_1/p_2 = \infty$. ○, calculated points.

integrating factor has been analytically evaluated for the results reported herein and that the numerical quadrature is considered more accurate than that used by Willis.

The average flow rates, non-dimensionalized with the upstream free-molecular values, are plotted in figure 3 versus the Reynolds number for pressure ratios of 2·0, 100 and infinity, and in figure 4 versus the pressure ratio for Reynolds numbers of 0, 0·05, 1·0 and 6·4. The results for $Re = 0$ correspond to the free-molecular values. The linearized expression for the average flow rate as given by Willis (1965) is also shown in figure 3. The constant a_2 was evaluated for a Reynolds number of 0·05. It is interesting to note that the best agreement occurs for the smallest pressure ratio and that the results for the full first iteration are always higher than the linearized results.

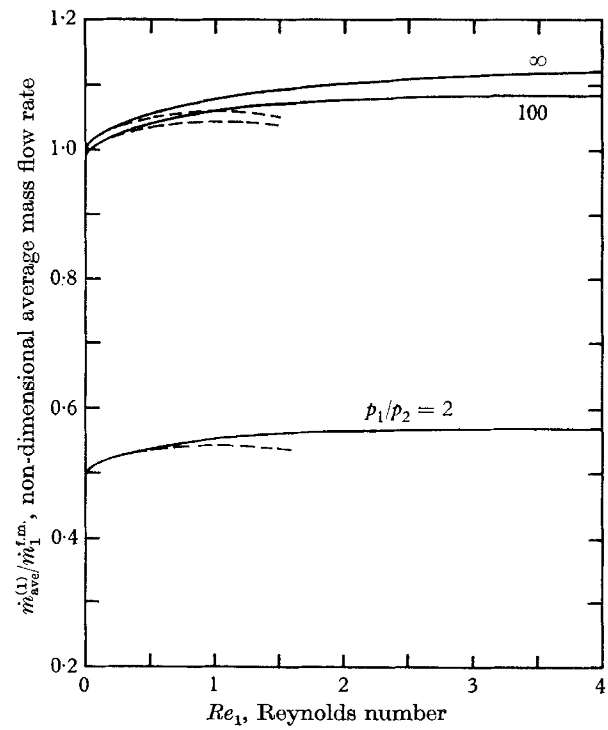

FIGURE 3. Non-dimensional average mass flow rate versus Reynolds number for several pressure ratios. — — —, $\dot{m}^{(1)}_{\text{ave}}/\dot{m}^{\text{f.m.}}_1 = \{1-(p_2/p_1)\}[1+a_2\alpha \log_e \alpha]$; $\alpha = Re_1/2\sqrt{2}$.

p_1/p_2	∞	100	2
a_2	$-0{\cdot}147$	$-0{\cdot}140$	$-0{\cdot}221$

It is apparent that the average flow rate increases with Reynolds number. Although it is not shown, a slight maximum occurred at a Reynolds number of approximately 4·5 for finite pressure ratios. However, the iterative method is specifically designed for small Reynolds numbers, so any conclusions drawn from the results for a Reynolds number of 4·5 or greater would be purely speculative. Note in figure 4 that the average flow rate increases quite rapidly for small pressure ratios and quite slowly for large pressure ratios. The maximum average flow rates for an infinite pressure ratio are also shown in figure 4 in order to illustrate how insensitive the average flow rate is with pressure ratio at large pressure ratios.

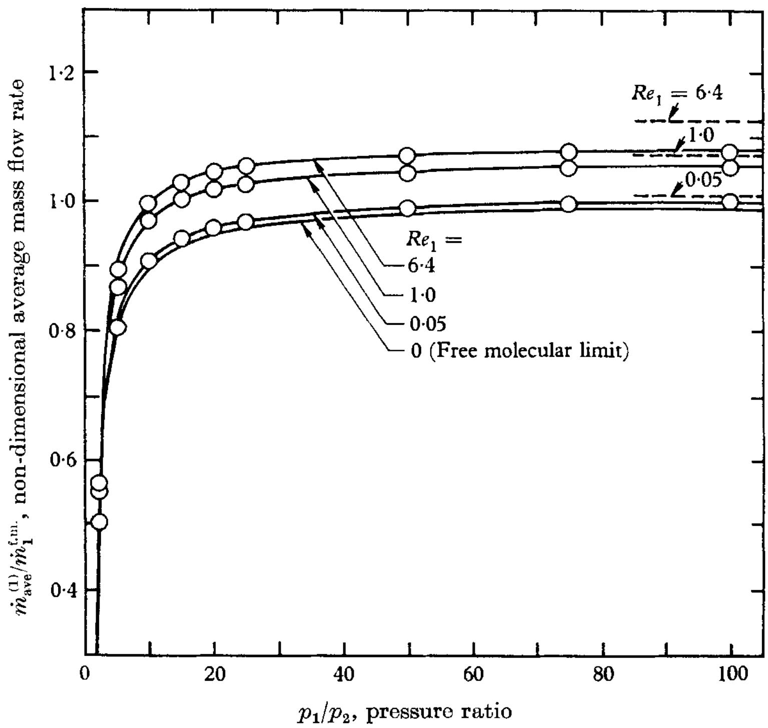

FIGURE 4. Non-dimensional average mass flow rate versus pressure ratio for several Reynolds numbers. ○, calculated points; — — —, vacuum limit, $p_1/p_2 = \infty$.

The non-dimensional average mass flow rate for an infinite Reynolds number has been calculated by Frankl (1947) for a specific heat ratio of 1·4. He obtains a value of 1·46. Note that this value is significantly higher than the nearly free molecular values presented in figures 3 and 4.

This work was in partial fulfillment of the Ph.D. degree in Aerospace Engineering at the Georgia Institute of Technology, Atlanta, Georgia, and was supported by NASA Research Grant NsG-657. The author wishes to express thanks to his thesis advisor Dr A. B. Huang for his valuable suggestions and assistance during the course of this study and to N. R. O'Brien, H. E. Wang and M. Epstein of the Aerospace Corporation for carefully reviewing the paper.

REFERENCES

BHATNAGER, P. L., GROSS, E. P. & KROOK, M. 1954 *Phys. Rev.* **94**, 511.
CHAHINE, M. T. & NARASIMHA, R. 1963 *Jet Propulsion Laboratory Rep.* no. 32–459.
FRANKL, F. I. 1947 *Trans. Acad. Sci., USSR* **58**, no. 3.
LIEPMANN, H. W. 1960 *J. Fluid Mech.* **10**, 65.
NARASIMHA, R. 1961 *J. Fluid Mech.* **10**, 371.

Stewart, J. D. 1967 Ph.D. Thesis, Georgia Institute of Technology, Atlanta, Georgia.

Willis, D. R. 1958 *Princeton University Aeronautical Engineering Laboratory Rep.* no. 440.

Willis, D. R. 1960 *Royal Institute of Technology, Kth Aero* TN 52.

Willis, D. R. 1964 *Princeton University Aeronautical Engineering Rep.* no. 683.

Willis, D. R. 1965 *J. Fluid Mech.* **21**, 21.